Supplementary Information of

Morphology control of self-organised $Sr_3V_2O_8$ nanostructures on $SrVO_3$ grown onto single and poly-crystalline subjacent $SrTiO_3$ substrates

Bruno Bérini[1], Marie Dallocchio[2], Adrian David[2], Ulrike Lüders[2], Yoan Bourlier[1], Ludivine Rault[3], Rosine Coq Germanicus[2], Wilfrid Prellier[2], Yves Dumont[1], Valérie Demange[3] and Arnaud Fouchet[2]

[1] Université Paris-Saclay, Université de Versailles Saint-Quentin, CNRS, GEMaC, 78000 Versailles, France

[2] Normandie Univ, ENSICAEN, UNICAEN, CNRS, CRISMAT, 14000 Caen, France

[3] Univ Rennes, CNRS, ISCR – UMR 6226, ScanMAT – UMS 2001, F-35000 Rennes, France

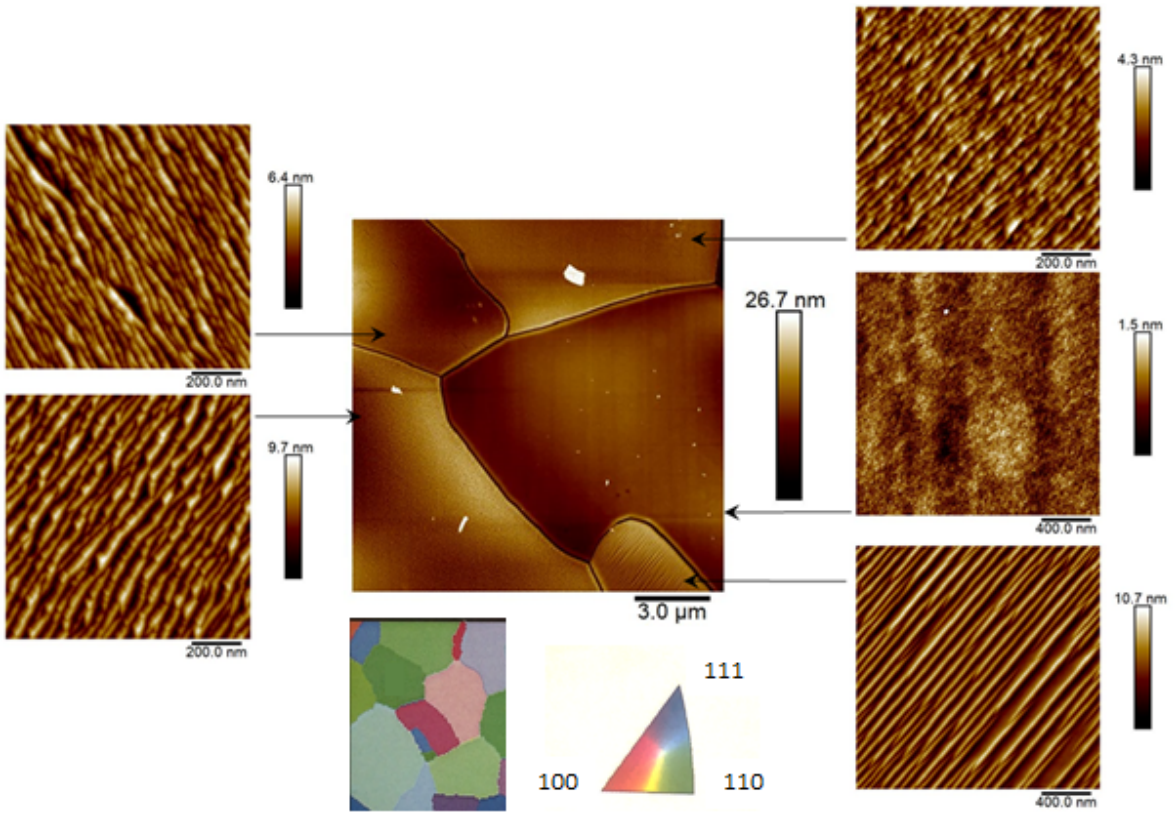

Figure SI-1. *AFM images of polycrystalline STO after cleaning (HF treatment) revealing the presence of terraces, and EBSD image of the same area.*

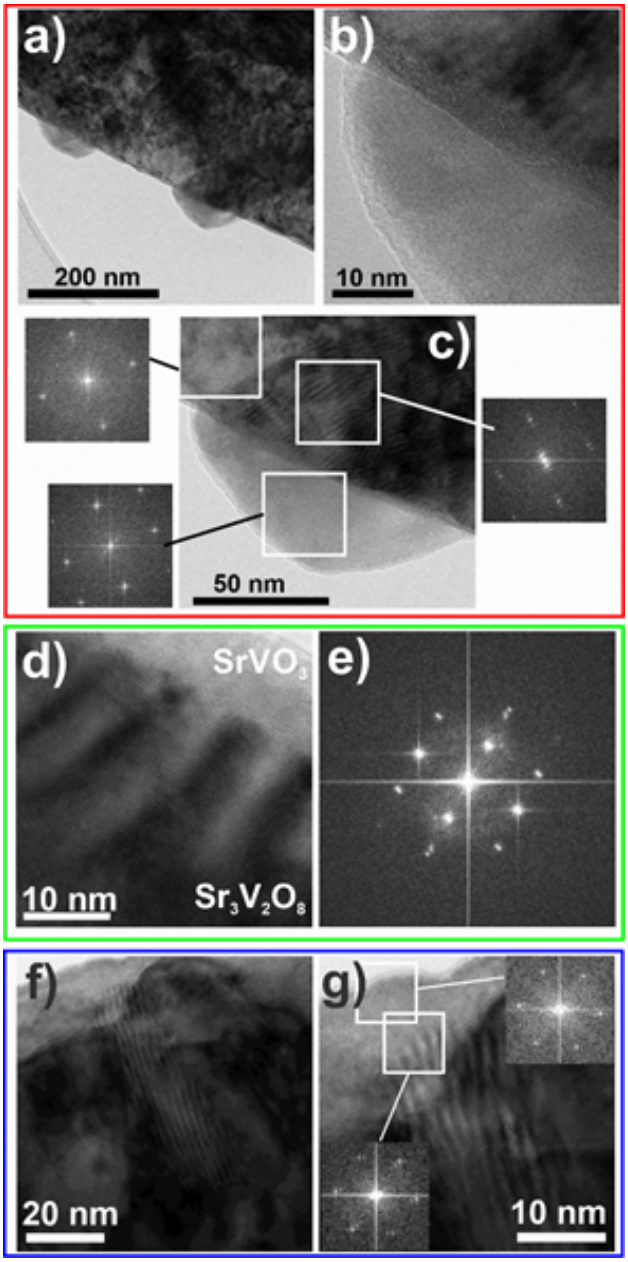

Figure SI-2. *a) Bright field TEM micrograph showing two $Sr_3V_2O_8$ NSs on the (100)SVO film. b) HRTEM image of one NS. c) HRTEM image of the same NS at lower magnification, showing Moiré fringes between the $Sr_3V_2O_8$ NS and the SVO film underneath, together with FFTs of 3 different areas (SVO film alone, $Sr_3V_2O_8$ NS alone, and $Sr_3V_2O_8$ on SVO) depicted by white squares. d) HRTEM image of one $Sr_3V_2O_8$ nanostructure on (110)SVO film showing Moiré fringes. e) FFT of the area displayed in (d). f) HRTEM image of one elongated $Sr_3V_2O_8$ NS on (111)SVO, displaying Moiré fringes. g) Same at higher magnification with FFT of SVO area and of $Sr_3V_2O_8$ area.*

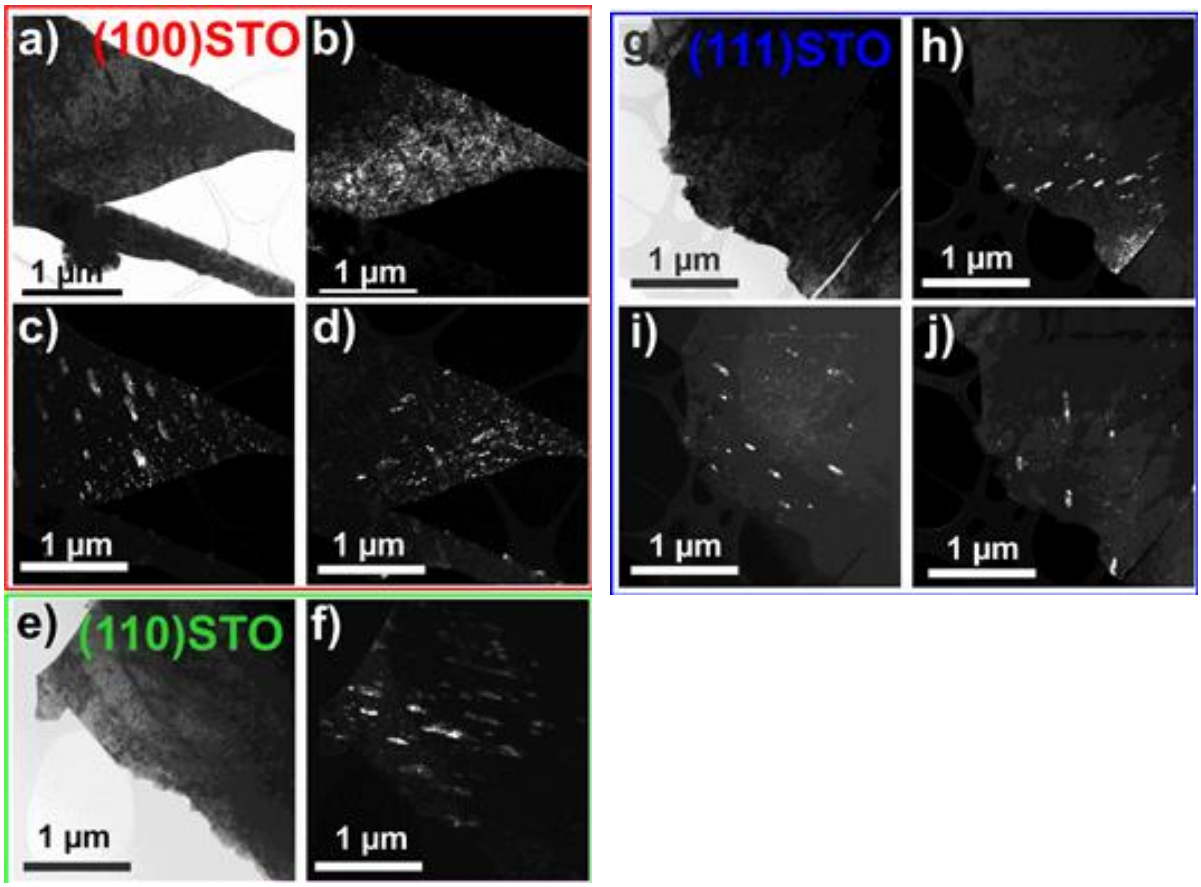

Figure SI-3. *a) Bright field TEM micrograph showing a plane view of a fragment of the (100)SVO film: the elongated NS have a dark contrast. b) Dark field TEM image of the same fragment obtained by selecting a fundamental SVO reflection: the perovskite phase is enlightened while the NS areas remain dark. c,d) Dark field TEM images obtained by selecting weak reflections of each* $Sr_3V_2O_8$ *variants showing them with a white contrast. e) Bright field TEM micrograph showing a plane view of a fragment of the (110)SVO film where some of the NS are seen with a dark contrast. f) Dark field TEM image of the same fragment obtained by selecting a weak reflection showing the NS with a light contrast. g) Bright field image of the (111)SVO film. h),i),j) Dark field images of the same area obtained by selecting reflections of each variant, showing the 3 possible orientations of the* $Sr_3V_2O_8$ *NS.*

Isotropic in plane NS on (100)SVO: 2 elongated nanostructures		Anisotropic in plane NS on (110)SVO: 1 elongated nanostructure	
Orientations	Lattice mismatch	Orientations	Lattice mismatch
(110) $Sr_3V_2O_8$// (011) SVO	-3.69%	(110)$Sr_3V_2O_8$ // (1-10)SVO	-3.69%
d(−11−5) $Sr_3V_2O_8$// d(01−1) SVO	-14.39%	(2-2-5)$Sr_3V_2O_8$ // (001)SVO	-8.33%

Isotropic in plane NS on (111)SVO: triangular nanostructure		Anisotropic in plane NS on (111)SVO: 3 elongated nanostructures	
Orientations	Lattice mismatch	Orientations	
(110)$Sr_3V_2O_8$ // (-110)SVO	-3.69%	(1-10)$Sr_3V_2O_8$ //(-110)SVO	-3.69%
(2-10)$Sr_3V_2O_8$ // (01-1)SVO	-3.69%	(-105)$Sr_3V_2O_8$ // (01-1)SVO	-14.39%

Table SI-1 listing the different lattice mismatches between the nanostructures and the SVO matrix.

Isotropic in plane NS on (100) SVO: 2 elongated nanostructures	Anisotropic in plane NS on (110) SVO: 1 elongated nanostructure	Isotropic in plane NS on (111) SVO: triangular nanostructure	Anisotropic in plane NS on (111) SVO: 3 elongated nanostructures
$Sr_3V_2O_8$ growth planes (110) and (1-15)	$Sr_3V_2O_8$ growth planes (110) and (-225)	$Sr_3V_2O_8$ growth planes (010), (1-10) and (100)	$Sr_3V_2O_8$ growth planes (110) and (-1 1 10)

Table SI-2 listing the different growth planes of the nanostructures extracted from TEM images.

a) b)

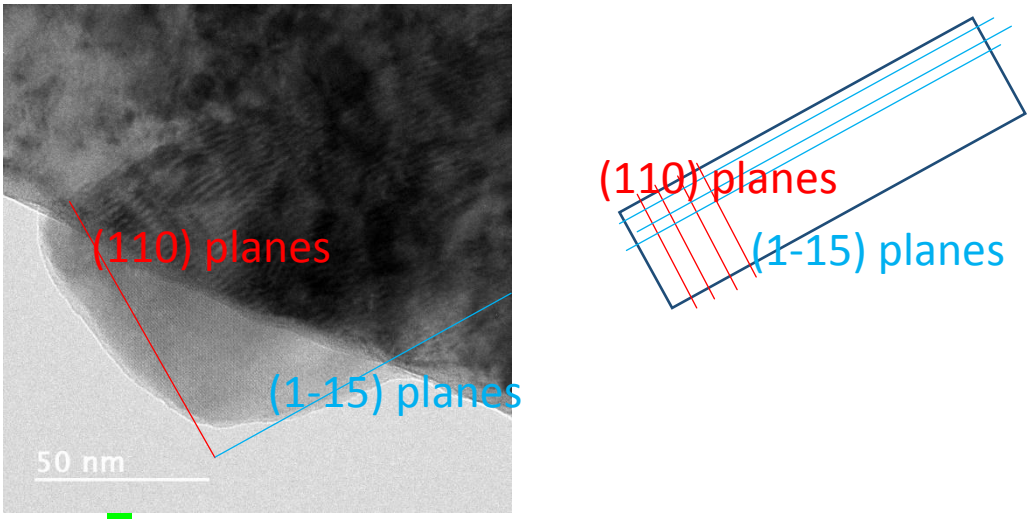

Fig. SI-4. *a) HRTEM image of the $Sr_3V_2O_8$ NS on the (100)SVO film with the orientations of the* growth planes *(from Figure SI_2b). b) Sketch of the nanostructure with its different* growth planes.

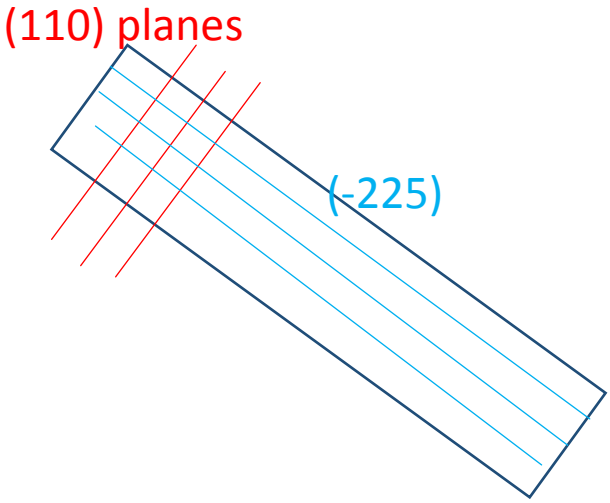

Fig. SI-5. *Sketch of the nanostructure of $Sr_3V_2O_8$ NS on the (110)SVO with its different* growth planes *(from Figure SI_2* d,e*).*

a)

b)

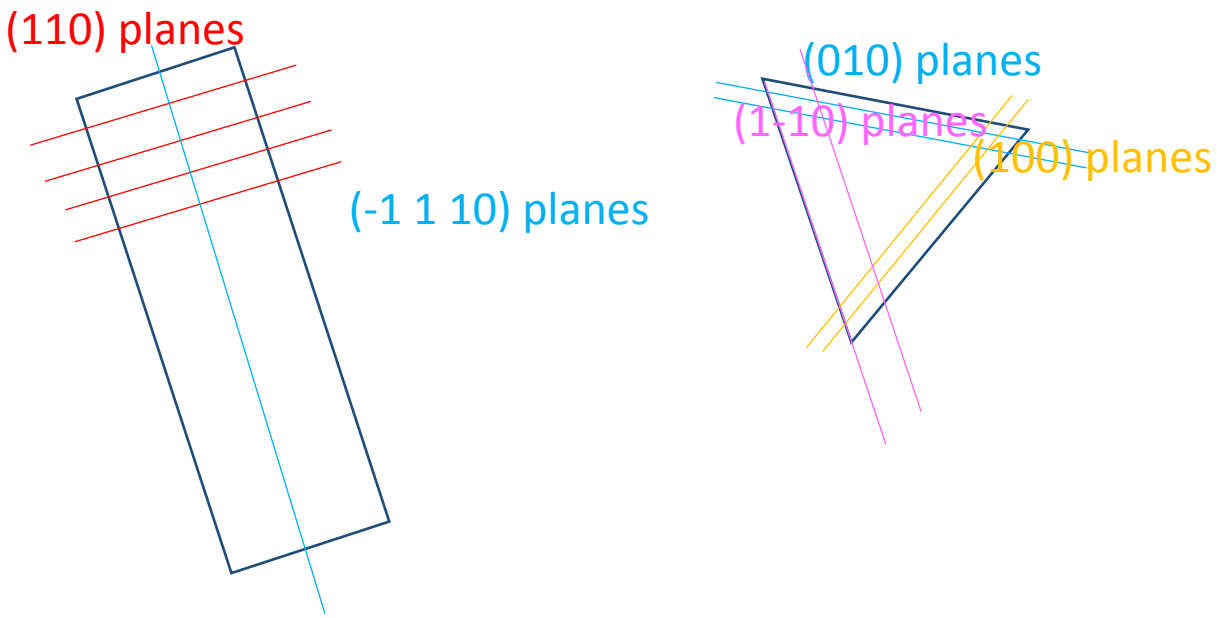

***Fig.* SI-6.** *Sketch of the nanostructures of $Sr_3V_2O_8$ NS on the (111)SVO with their different* growth planes *for the elongated one (a) (from Figure SI_2 f,g) and triangular one (b) from (figure 5a-b).*

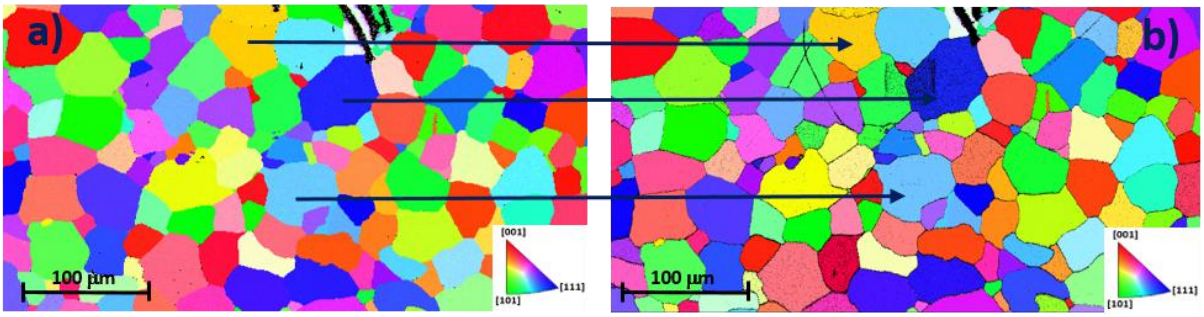

Figure SI-7. *EBSD maps of the polycrystalline STO substrate (inset: stereographic orientation) (a) and of the same area after growth of the SVO 40 nm thick film (b).*

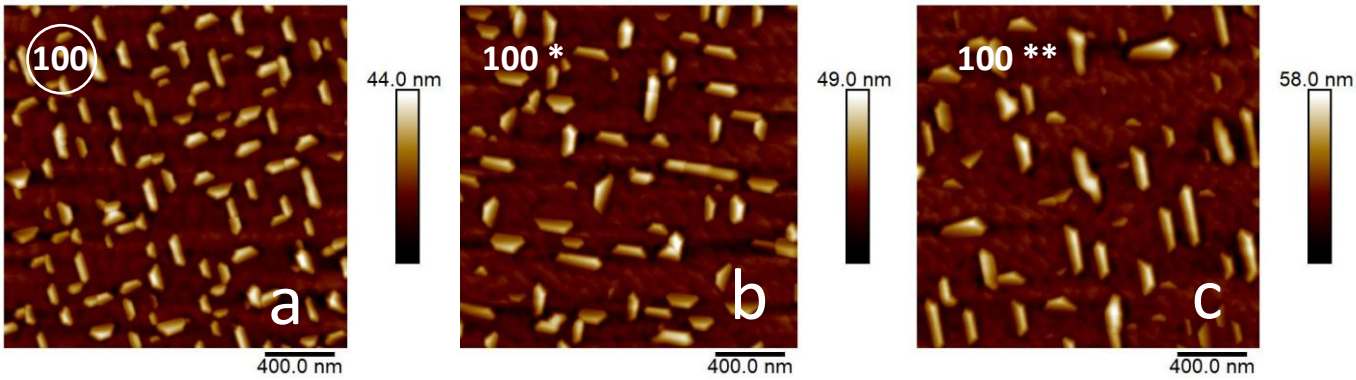

Figure SI-8. *AFM images of three (100) oriented STO grains of the polycrystalline substrate (cf. red color on figure 6).*

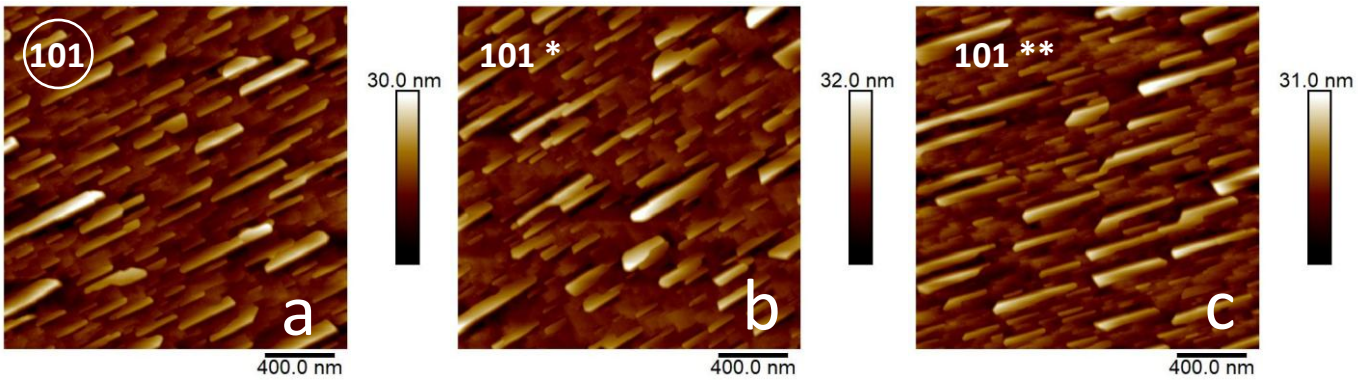

Figure SI-9. *AFM images of three (110) oriented STO grains of the polycrystalline substrate (cf. green color on figure 6).*

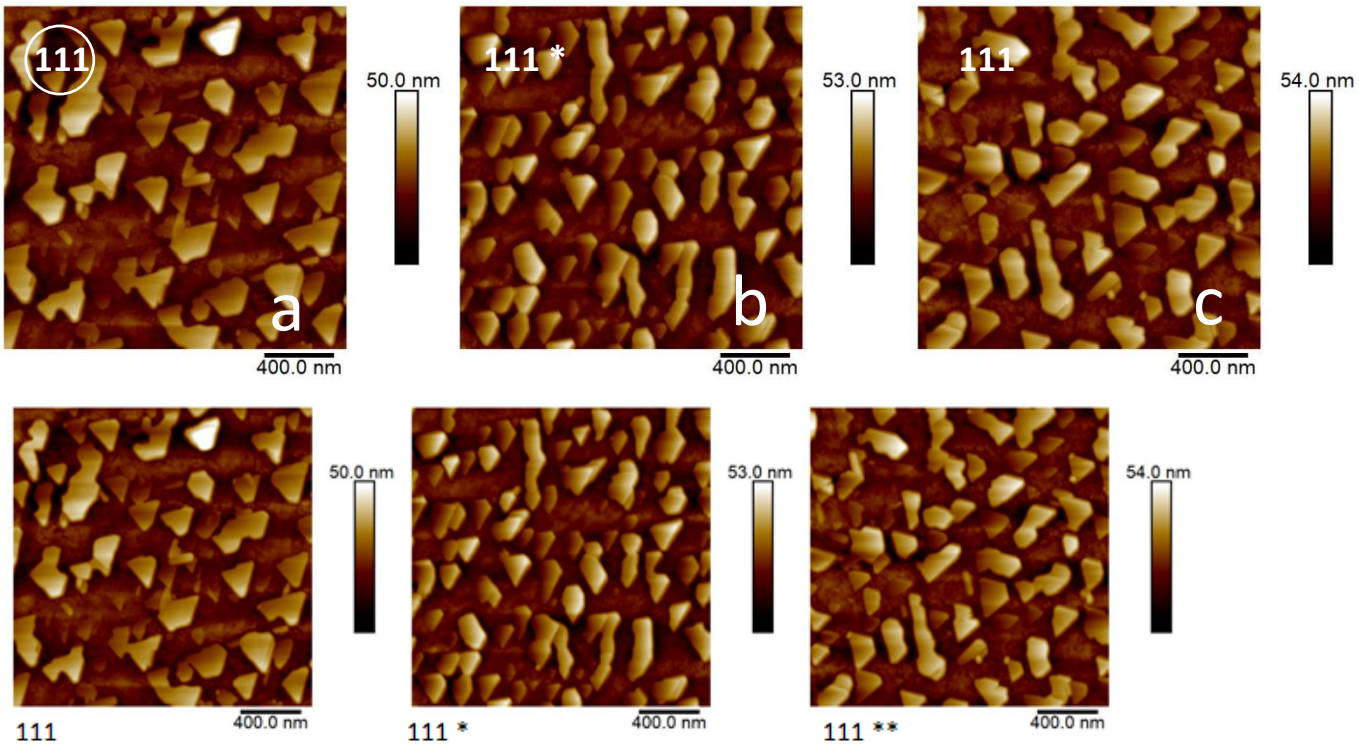

Figure SI-10. *AFM images of three (111) oriented STO grains of the polycrystalline substrate (cf. blue color on figure 6).*

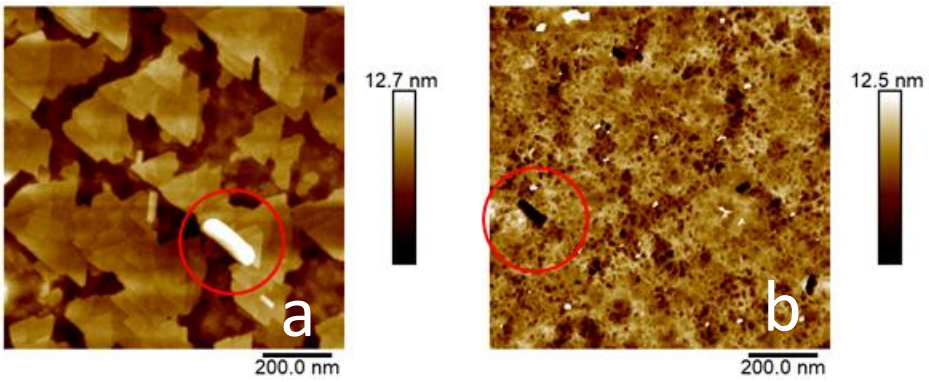

Figure SI-11. *AFM images of SVO film grown on single crystalline (111) substrate after NS dissolution for 60 s. The red circle depicts the same elongated NS before (a) and after (b) dissolution.*